Journal of Power Sources 251 (2014) 108–112

Contents lists available at ScienceDirect

Journal of Power Sources

journal homepage: www.elsevier.com/locate/jpowsour

Short communication

An electrochemical device with a multifunctional sensor for gas diffusivity measurement in fuel cells

Weidong He [a,*], John B. Goodenough [b]

[a] School of Energy Science and Engineering, University of Electronic Science and Technology of China (UESTC), Chengdu 611731, PR China
[b] Texas Materials Institute, ETC 9.102, The University of Texas at Austin, Austin, TX 78712, USA

HIGHLIGHTS

- Designs a multifunctional sensor device for accurate diffusivity measurement.
- Eliminates temperature uncertainty in the diffusivity measurement.
- Improves efficiency of evaluating concentration polarization & limiting current.

GRAPHICAL ABSTRACT

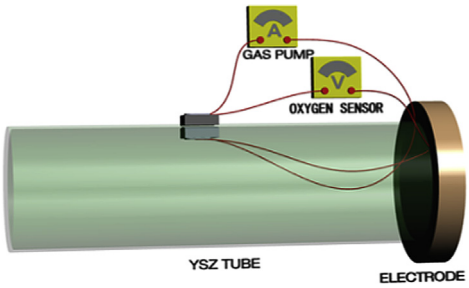

ARTICLE INFO

Article history:
Received 1 October 2013
Received in revised form
30 October 2013
Accepted 14 November 2013
Available online 1 December 2013

Keywords:
Fuel cells
Oxygen sensors
Diffusivities
Limiting current densities
Electrode thicknesses
Concentration polarizations

ABSTRACT

Mass transport is of paramount importance to the electrochemical performance of fuel cells. The high performance of fuel cells requires a large diffusion coefficient, *i.e.* the diffusivity, of the gas transport in electrodes and efficient gas diffusion can lead to large limiting currents and controlled concentration polarization. Recently-designed electrochemical devices allow for the direct evaluation of gas diffusivity in fuel cells. To realize these devices, a gas pump and an oxygen sensor are typically attached to two different spots of the inside wall of an electrolyte tube, which inevitably induces the uncertainty in measurement temperature. To eliminate temperature uncertainty in the diffusivity measurement, an electrochemical device with a multifunctional sensor is designed in this report. Quantitative analysis shows that temperature uncertainty can indeed induce substantial evaluation errors of gas diffusivity, limiting current density and concentration polarization, which in turn verifies the necessity of the multifunctional sensor device for the accurate diffusivity measurement in fuel cells.

1. Introduction

The high performance of fuel cells requires efficient mass transport in the electrolytes and the porous electrodes. To acquire efficient mass transport, the conduction of ionic species and the diffusion of gaseous fuel species must be fast [1–3]. In recent years, it has become the key focus in the fuel cell field, especially in the solid oxide fuel cell (SOFC) area, to develop fuel cell materials that exhibit improved conduction and diffusion properties at relatively low operation temperatures [4,5]. Such efforts have resulted in tremendous scientific findings in the fuel cell area and have brought about insightful implications in the general energy area. For instance, Santamaria et al. reported the colossal conductivity at the interfaces of crystalline ZrO_2:Y_2O_3/$SrTiO_3$ heterostructures [6]. Vertically-aligned nanocomposite material $(Ce_{0.9}Gd_{0.1}O_{1.95})_{0.5}$/$(Zr_{0.92}Y_{0.08}O_{1.96})_{0.5}$(GDC/YSZ) with pronounced ionic conductivity was realized via a PLD method by Wang et al [7]. To achieve fast

* Corresponding author. Tel./fax: +86 28 61831252.
E-mail address: weidong.he@uestc.edu.cn (W. He).

0378-7753/$ – see front matter © 2013 Elsevier B.V. All rights reserved.
http://dx.doi.org/10.1016/j.jpowsour.2013.11.061

diffusion at a low operating temperature, Hussain et al. prepared nickel-ceria infiltrated Nb-doped $SrTiO_3$ anodes with highly-efficient diffusion properties [8]. Park et al. employed a screen-printing method to synthesize (La, Sr)CoO_3-based multilayered composite cathode materials that exhibit pronounced transport properties [9]. In parallel, the techniques for the measurement of mass transport in fuel cells have also been well advanced in recent years [10–12]. In particular, the authors have designed sensor-based electrochemical devices for the direct measurement of gas diffusivity in fuel cells [13–18]. The measured gas diffusivity provides the quantitative basis for the efficient evaluation of limiting current density and concentration polarization, which are two key performance parameters in fuel cells. However, all the previous electrochemical devices designed by the authors neglected the temperature uncertainty caused by the different positions of the oxygen pump and the oxygen sensor across the electrolyte tube. As a consequence, errors in the gas diffusivity measurement and the subsequent evaluations of limiting current and concentration polarization were inevitably induced according to Eqs. 1–6,

$$\Delta D^{\mathrm{eff}}_{\mathrm{H_2-H_2O}} = \frac{RTl_{\mathrm{a}}i}{4F\left(p^{\mathrm{o}}_{\mathrm{H_2}} - \Delta p^{\mathrm{i}}_{\mathrm{H_2}}\right)} \tag{1}$$

$$\Delta D^{\mathrm{eff}}_{\mathrm{O_2-N_2}} = \frac{RTl_{\mathrm{c}}i}{8F\left(\Delta p^{\mathrm{i}}_{\mathrm{O_2}} - p^{\mathrm{o}}_{\mathrm{O_2}}\right)} \tag{2}$$

where T is the measurement temperature, F is the Faraday constant, R is the gas constant, i is the applied current density, l_{a} (l_{c}) is the anode (cathode) thickness, $D^{\mathrm{eff}}_{\mathrm{H_2-H_2O}}(D^{\mathrm{eff}}_{\mathrm{O_2-N_2}})$ is the effective binary gas diffusivity of the anode (cathode), $p^{\mathrm{o}}_{\mathrm{H_2}}(p^{\mathrm{o}}_{\mathrm{O_2}})$ is the H_2 (O_2) pressure out of the measurement device, and $p^{\mathrm{i}}_{\mathrm{H_2}}a(p^{\mathrm{i}}_{\mathrm{O_2}})$ is the H_2 (O_2) pressure in the YSZ tube of the device [13–18].

$$i_{\mathrm{a}} \approx \frac{4Fp^{\mathrm{o}}_{\mathrm{H_2}}D^{\mathrm{eff}}_{\mathrm{H_2-H_2O}}}{RTl_{\mathrm{a}}} \tag{3}$$

$$i_{\mathrm{c}} \approx \frac{8Fp^{\mathrm{o}}_{\mathrm{O_2}}D^{\mathrm{eff}}_{\mathrm{O_2-N_2}}}{RTl_{\mathrm{c}}}\left(\frac{p_{\mathrm{t}}}{p_{\mathrm{t}} - p^{\mathrm{o}}_{\mathrm{O_2}}}\right) \tag{4}$$

where i_{a} (i_{c}) is the anode (cathode) limiting current density, and p_{t} ($\sim$1 atm) is the total pressure of gaseous species in the measurement system.

$$\eta_{\mathrm{a}} = -\frac{RT}{2F}\ln\left(1 - \frac{i}{i_{\mathrm{a}}}\right) + \frac{RT}{2F}\ln\left(1 + \frac{p^{\mathrm{o}}_{\mathrm{H_2}}i}{p^{\mathrm{o}}_{\mathrm{H_2O}}i_{\mathrm{a}}}\right) \tag{5}$$

$$\eta_{\mathrm{c}} = -\frac{RT}{4F}\ln\left(1 - \frac{i}{i_{\mathrm{c}}}\right) \tag{6}$$

where η_{a} (η_{c}) is the concentration polarization of the anode (cathode), and $p^{\mathrm{o}}_{\mathrm{H_2}}(p^{\mathrm{o}}_{\mathrm{H_2O}})$ is the pressure of the anode gas (H_2–H_2O) [13–15].

In this report, we eliminate the temperature uncertainty in the gas diffusivity measurement in fuel cells by proposing an electrochemical device with a multifunctional sensor. Our analysis shows that the electrochemical device largely improves the accuracy in the direct gas diffusivity measurement and the evaluations of limiting current and concentration polarization. The device along with the quantitative analysis is expected to facilitate the development of low-temperature fuel cells with reduced energy loss.

2. Materials and methods

2.1. Multifunctional-sensor electrochemical cell device

The electrochemical device proposed for the diffusivity measurement in solid oxide fuel cells is shown in Fig. 1. Without special notes, all the following results and discussions in this report are centered on solid oxide fuel cells. In principle, the device can be employed for the diffusivity measurement in any type of fuel cells upon adjustment of the electrolyte and electrode materials in the device. The proposed device, as shown in Fig. 1, exhibits two obvious advantages over previous electrochemical devices for the gas diffusivity measurement in fuel cells. First, in the previous electrochemical devices, electrolyte discs were attached to the ends of the electrolyte tubes, which could cause gas leak in the diffusivity measurement. Furthermore, the electrolyte discs were typically obtained *via* complex treatments including die pressing, polishing and high-temperature annealing, etc. The employment of the electrolyte disc on one end of the electrolyte tube in the proposed electrochemical device is avoided. The basic frame of the electrochemical device only consists of an electrode to be measured and an electrolyte tube with only one open end and thus, the device is much simplified compared to the previous electrochemical devices. Second, the oxygen sensor and the oxygen pump are located at the same spot across the electrolyte tube. Therefore, the oxygen pump and the oxygen sensor can be operated at the same temperature, and as a result the temperature uncertainty in the diffusivity measurement is eliminated.

2.2. Theoretical analysis for cathode diffusivity measurement

The working mechanisms of anode and cathode diffusivity measurements are similar, and for simplicity we here analyze the working principle of the cathode diffusivity measurement [10]. In the cathode diffusivity measurement, the proposed electrochemical device is placed at the center of a tube furnace and purged with O_2–N_2 gas mixture. With an applied current *via* the oxygen pump (Fig. 1) in an O_2–N_2 flow at a fixed flow rate, a flux of O_2–N_2 gas mixture is induced through the porous cathode sample (Fig. 1) according to the Faraday's law, and the correlation between the flux and the applied current is expressed in Eq. (7),

$$J_{O2} = \frac{i}{4F} \tag{7}$$

where J_{O2} is the O_2 flux induced by the applied current i. Such an induced gas flux results in the pressure difference inside and out of the proposed electrochemical device in the tube furnace. After

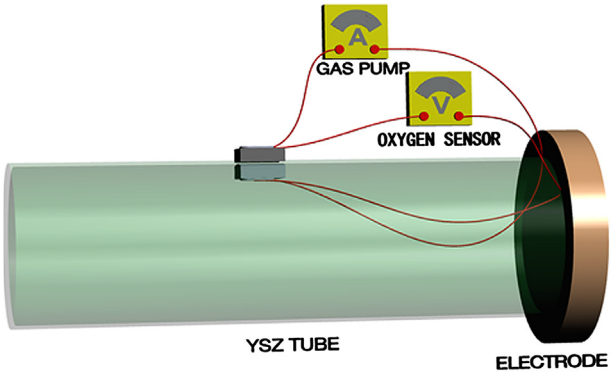

Fig. 1. An electrochemical device with a multifunctional sensor for accurate gas diffusivity measurement in fuel cells. The operation mechanism is based on Eqs. 1–6 and the equilibrium gas reaction of $2H_2O(g) \Leftrightarrow 2H_2(g) + O_2(g)$.

~10 min, the gas phases inside and out of the electrochemical device in a tube furnace reach an equilibrium state driven by the pressure difference inside and out of the proposed electrochemical device. At such an equilibrium state, switching the operation of the oxygen pump over to the operation of the oxygen sensor allows for the measurement of a decaying voltage as demonstrated in Fig. S1. Based on the applied current, the initial voltage and the reaction constant for three-phase reaction $2H_2O(g) \Leftrightarrow 2H_2(g) + O_2(g)$, the cathode gas diffusivity $D^{eff}_{O_2-N_2}$ can then be determined via Eq. (2). In the case of measuring the anode gas diffusivity, the gas flow, the electrode sample and metal wirings for electrical connection need to be adjusted accordingly. Clearly, this method of measuring gas diffusivity in fuel cells is much simplified and more efficient compared to the previous measurement techniques. Next, we perform quantitative analysis to justify the necessity of the proposed electrochemical device for the accurate gas diffusivity measurement in fuel cells. The dimensions of such electrochemical devices are typically within 0.2 m. The temperature variance within 0.2 m range can be different for various furnace systems, but is expected to lie in the range of 0–100 °C in the diffusivity measurement in fuel cells with working temperatures above 500 °C. In the following analysis, we thus allow the temperature uncertainty to vary within the range of 0–20%.

3. Results and discussion

The evaluation error ΔD induced by the temperature variance ΔT can be calculated with known applied current density and electrode thickness based on Eqs. (1) and (2). As shown in Fig. 2, for both anodes (Fig. 2a) and cathodes (Fig. 2b), ΔD increases linearly with increasing ΔT as $\Delta T/T$ varies in the range of 0–20%. The relatively steep slopes of the ΔD plots for the different temperatures suggest that an uncertainty in the temperature indeed induces substantial errors in the gas diffusivity evaluation. With a certain temperature uncertainty, for both electrodes the temperature uncertainty for high-temperature measurements results in larger evaluation errors compared to the evaluation errors for low-temperature measurements; with a fixed value of temperature uncertainty, the error of the diffusivity evaluation for measurement temperature 800 °C is the largest among the four considered measurement temperatures, followed by the errors of the diffusivity evaluation for measurement temperatures 750 °C, 700 °C and 650 °C, respectively, as shown in Fig. 2a and b. Thus the temperature uncertainty is more disastrous for the gas diffusivity evaluation of high-temperature fuel cells. The proposed device is highly desirable for SOFCs since the working temperatures of currently-existing SOFCs are typically above 500 °C.

As shown in Eqs. (3) and (4), limiting current is quantitatively correlated with gas diffusivity. We thus evaluate the error in the evaluation of limiting current density as a function of temperature uncertainty in the gas diffusivity measurement of fuel cells. Δi_a (Δi_c) is linearly increasing with increasing $\Delta T/T$ as shown in Fig. 3. For anodes, Δi_a appears to be less dependent on temperature in the medium temperature range compared to the Δi_a at low and high temperatures, as noted by the close magnitudes of Δi_a at 700 °C and 750 °C. Δi_c increases sharply with increasing $\Delta T/T$ at any temperature as noted by the almost overlapping plots of Δi_c *versus* $\Delta T/T$, as shown in Fig. 3b. Unlike the monotonous increase in the evaluation error of limiting current density with increasing measurement temperature, the evaluation error of cathode limiting current density exhibits an irregular dependence on electrode thickness although Δi_a (Δi_c) increases with increasing $\Delta T/T$ for all the considered electrode thicknesses in Fig. 3c and d. For instance, with a fixed temperature uncertainty the evaluation error of limiting current density is the largest for

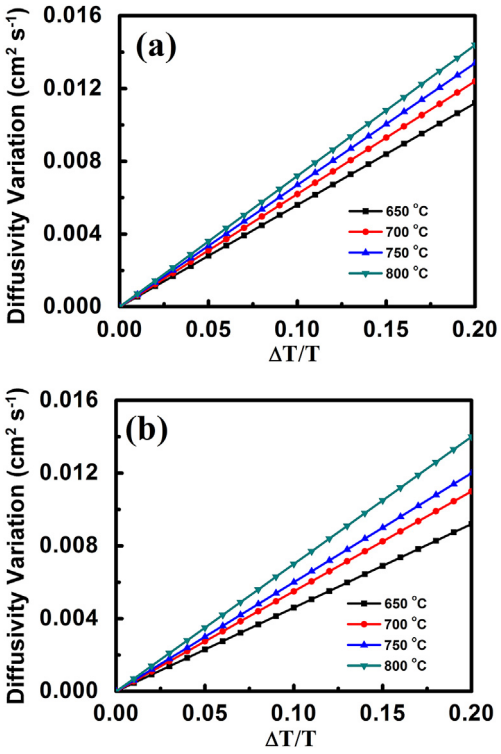

Fig. 2. Plots of anode (a) and cathode (b) diffusivity measurement errors as a function of the uncertainty in measurement temperature ($\Delta T/T$) with an applied current density of 500 A m^{-2}. Anode hydrogen effective binary diffusivities are 0.046 cm^2 s^{-1} for 650 °C, 0.055 cm^2 s^{-1} for 700 °C, 0.06 cm^2 s^{-1} for 750 °C and 0.07 cm^2 s^{-1} for 800 °C, respectively. Cathode oxygen effective binary diffusivities are 0.056 cm^2 s^{-1} for 650 °C, 0.062 cm^2 s^{-1} for 700 °C, 0.067 cm^2 s^{-1} for 750 °C, and 0.072 cm^2 s^{-1} for 800 °C, respectively. Anode thickness is 0.75 mm and cathode thickness is 0.2 mm.

0.2 mm cathodes, followed by 2 mm, 20 nm and 2 μm cathodes, respectively; however, no irregularity is observed in the Log (Δi_a)-*versus*-$\Delta T/T$ plots for anodes with various thicknesses at 700 °C. The irregular cathode thickness dependence suggests that eliminating the temperature uncertainty in the diffusivity measurement in fuel cells is necessary for any cathode thickness and that the effort of achieving accurate gas diffusivity measurement *via* the previous electrochemical devices by selecting certain electrode thicknesses is not viable.

Both diffusivity and limiting current interplay quantitatively with the concentration polarization of fuel cells, a major source of polarizations in fuel cells with electrodes characterized with impeded gas transport [19–21]. To further evaluate the necessity of the multifunctional sensor electrochemical device as proposed in this report, we then analyze the evaluation of concentration polarization as a function of temperature uncertainty at different measurement temperatures and for electrodes of different thicknesses. ΔCP increases with increasing temperature uncertainty in all the ΔCP-*versus*-$\Delta T/T$ plots for anodes and cathodes at different temperatures and for different electrode thicknesses, as shown in Fig. 4. Interestingly, unlike the plots of diffusivity and limiting current density evaluation errors in Figs. 2 and 3, the concentration polarization evaluation error exhibits an irregular dependence on the measurement temperature for anodes. For instance, with a fixed temperature uncertainty the evaluation error of anode concentration polarization at 650 °C is the largest among the four considered temperatures, followed by the evaluation error of anode concentration polarization at 750 °C, 800 °C, and 700 °C, respectively, as shown in Fig. 4a. Further, irregular electrode thickness dependence is also observed in the Log (ΔCP)-*versus*-$\Delta T/T$ plots for

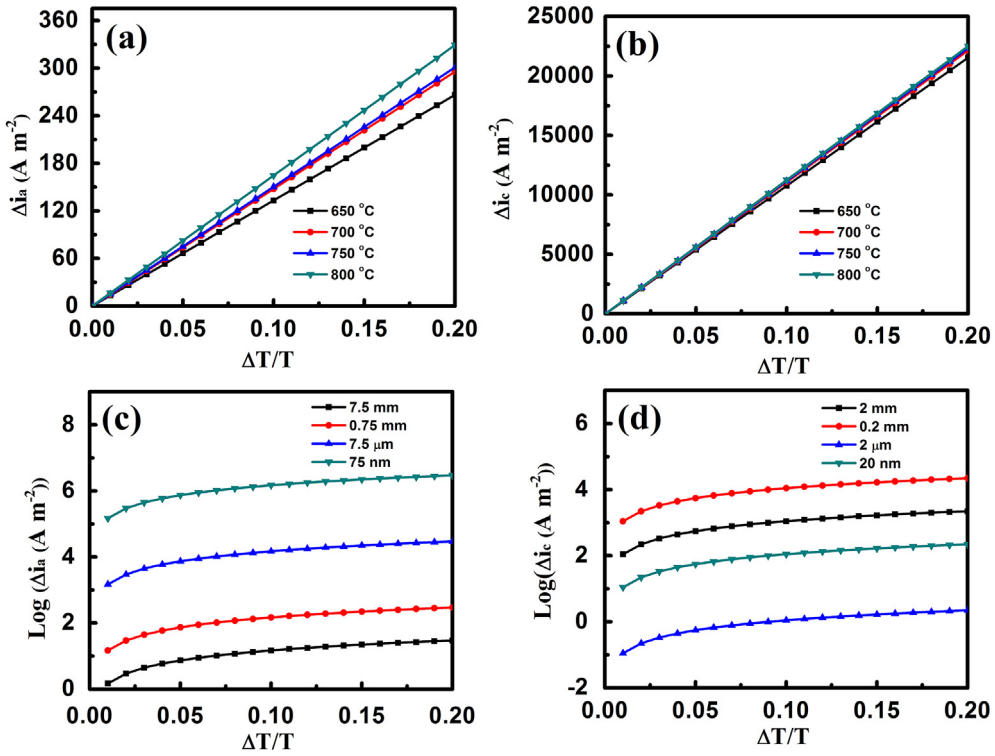

Fig. 3. Plots of the evaluation errors in anode (a) and cathode (b) limiting current density as a function of the measurement temperature uncertainty ($\Delta T/T$) with an applied current density of 500 A m^{-2}. Anode thickness is 0.75 mm and cathode thickness is 0.2 mm. Anode limiting current densities are 1.33×10^3 A m^{-2} for 650 °C, 1.48×10^3 A m^{-2} for 700 °C, 1.51×10^3 A m^{-2} for 750 °C and 1.65×10^3 A m^{-2} for 800 °C, respectively. Cathode limiting current densities are 10.77×10^4 A m^{-2} for 650 °C, 11.07×10^4 A m^{-2} for 700 °C, 11.17×10^4 A m^{-2} for 750 °C and 11.25×10^4 A m^{-2} for 800 °C, respectively. Log (Δi_a) (Log (Δi_c))-*versus*-$\Delta T/T$ plots for different electrode thicknesses at 700 °C and with an applied current density of 500 A m^{-2}.

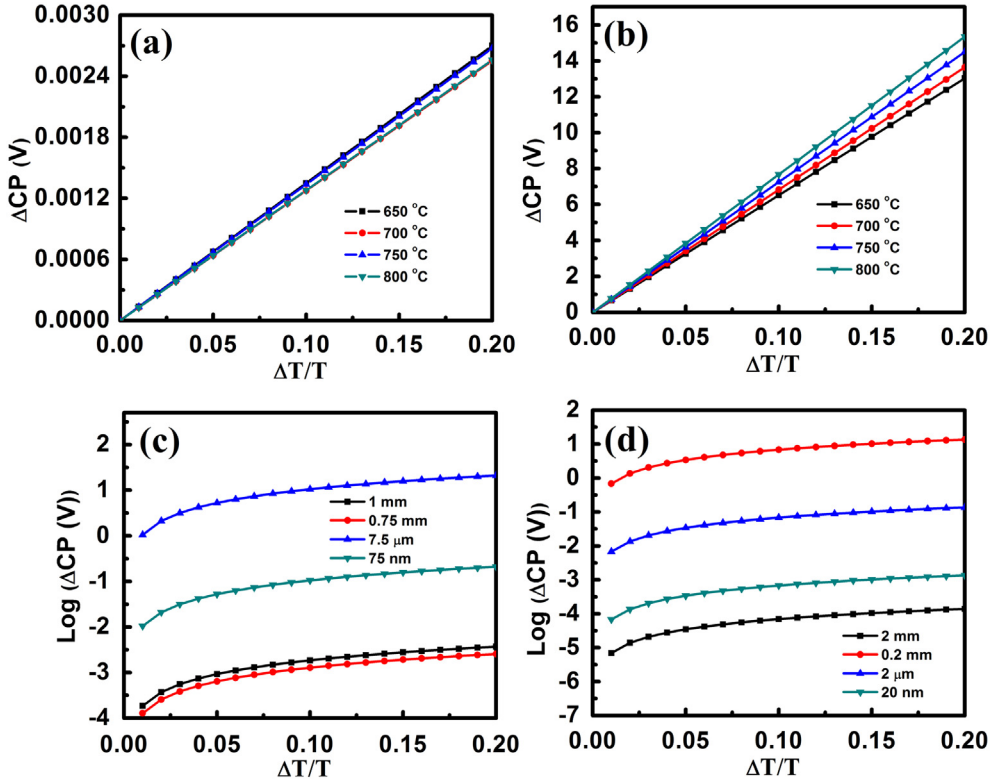

Fig. 4. Plots of the evaluation errors in the anode (a) and cathode (b) concentration polarization as a function of the uncertainty ($\Delta T/T$) in measurement temperature. Anode concentration polarizations are 0.0128 V for 650 °C, 0.0134 V for 700 °C, 0.0128 V for 750 °C and 0.0135 V for 800 °C, respectively. Cathode concentration polarizations are 6.5×10^{-4} V for 650 °C, 6.8×10^{-4} V for 700 °C, 7.2×10^{-4} V for 750 °C and 7.7×10^{-4} V for 800 °C, respectively. Log (ΔCP)-*versus*-$\Delta T/T$ plots for different electrode thicknesses at 700 °C and with an applied current density of 500 A m^{-2}. Anode thickness is 0.75 mm and cathode thickness is 0.2 mm.

different anode (cathode) thicknesses at 700 °C. The irregular dependences of concentration polarization on the measurement temperature and the electrode thicknesses further confirm the necessity of eliminating the temperature uncertainty in the gas diffusivity measurement in fuel cells. Therefore, the proposed electrochemical device is highly-desirable for the gas diffusivity measurement in both bulk and thin nanostructured fuel cell systems operated at any temperature.

In the above analysis, different thicknesses and certain applied current densities are chosen for anodes and cathodes for direct comparison with the authors' previous experimental and theoretical results [10]. Further detailed insight into thickness/current density dependences can be readily obtained according to the systematic investigation into the thickness/current density dependences in the authors' previous reports [14–17].

In conclusion, a multifunctional sensor electrochemical device is proposed for the accurate gas diffusivity measurement in fuel cells. With the device, the temperature uncertainty, which induces substantial errors in the evaluations of limiting current density and concentration polarization, can be eliminated in the gas diffusivity measurement in fuel cells. Our quantitative analysis suggests that the elimination of the temperature uncertainty is necessary in the diffusivity measurement in both bulk and thin nanostructured fuel cells at any operating temperature. Our proposed device along with the quantitative analysis facilitates the development of low-temperature fuel cells with low energy loss.

Acknowledgments

The work is supported by the UESTC new faculty startup fund. The author thanks Kechun Wang and Yu Wan for their help with the quantitative analysis.

Appendix A. Supplementary data

Supplementary data related to this article can be found at http://dx.doi.org/10.1016/j.jpowsour.2013.11.061.

References

[1] J.W. Kim, A.V. Virkar, K.Z. Fung, K. Mehta, S.C. Singhal, J. Electrochem. Soc. 146 (1999) 69–78.
[2] Z.P. Shao, S.M. Haile, Nature 431 (2004) 170–173.
[3] S.H. Chan, K.A. Khor, Z.T. Xia, J. Power Sources 93 (2001) 130–140.
[4] B.C.H. Steele, A. Heinzel, Nature 414 (2001) 345–352.
[5] L. Cindrella, et al., J Power Sources 194 (2009) 146–160.
[6] J.G. Barriocanal, A.R. Calzada, M. Varela, Z. Sefrioui, E. Iborra, C. Leon, S.J. Pennycook, J. Santamaria, Science 321 (2008) 676–680.
[7] Q. Su, D. Yoon, A. Chen, F. Khatkhatay, A. Manthiram, H. Wang, J. Power Sources 242 (2013) 455–463.
[8] A.M. Hussain, J.V.T. Høgh, T. Jacobsen, N. Bonanos, Int. J. Hydrogen Energy 37 (2012) 4309–4318.
[9] S.-Y. Park, H. Ji, H.-R. Kim, K.J. Yoon, J.-W. Son, B.-K. Kim, H.-J. Je, H.-W. Lee, J.-H. Lee, J. Power Sources 228 (2013) 97–103.
[10] W. He, B. Wang, J. Power Sources 232 (2013) 93–98.
[11] Z. Yu, R.N. Carter, J. Power Sources 195 (2010) 1079–1084.
[12] C. Chan, N. Zamel, X. Li, J. Shen, Electrochim. Acta 65 (2012) 13–21.
[13] W. He, J. Zou, B. Wang, et al., J. Power Sources 237 (2013) 64–73.
[14] W. He, K.J. Yoon, R.S. Eriksen, et al., J. Power Sources 195 (2010) 532–535.
[15] W. He, B. Wang, H. Zhao, et al., J. Power Sources 196 (2011) 9985–9988.
[16] W. He, B. Wang, Adv. Energy Mater. 2 (2012) 329–333.
[17] W. He, B. Wang, J.H. Dickerson, Nano Energy 1 (2012) 328–332.
[18] W. He, X. Lin, J.H. Dickerson, J.B. Goodenough, Nano Energy 2 (2013) 1004–1009.
[19] Z. Lin, G. Waller, Y. Liu, M. Liu, C.P. Wong, Adv. Energy Mater. 2 (2012) 884–888.
[20] T. Howells, E. New, P. Sullivan, T.S. Jones, Adv. Energy Mater. 1 (2011) 1085–1088.
[21] J.R. Moore, S.A. Seifried, A. Rao, S. Massip, B. Watts, D.J. Morgan, R.H. Friend, C.R. McNeill, H. Sirringhaus, Adv. Energy Mater. 1 (2011) 230–240.